Korean J. Chem. Eng., **27**(2), 632-638 (2010)
DOI: 10.1007/s11814-010-0079-9

Breakthrough data analysis of adsorption of volatile organic compounds on granular activated carbon

Kwang-Joong Oh*, Dae-Won Park*, Seong-Soo Kim, and Sang-Wook Park*,†**

*Division of Chemical Engineering, Pusan National University, Busan 609-735, Korea
**School of Environmental Science, Catholic University of Pusan, Busan 609-757, Korea
(*Received 2 July 2009 • accepted 19 August 2009*)

Abstract−Volatile Organic Compounds (VOCs) such as methanol, ethanol, methyl ethyl keton, benzene, n-propanol, toluene, and o-xylene were adsorbed in a laboratory-scale packed-bed adsorber using granular activated carbon (GAC) at 101.3 kPa. The adsorber was operated batchwise to obtain the breakthrough curves of VOCs under the adsorption conditions such as adsorption temperatures (298-323 K), flow rates of nitrogen (60×10^{-6}-150×10^{-6} m^3/min), GAC amount of 0.002 kg, and concentration of VOCs (3,000-6,000 ppmv). The adsorption kinetics was obtained by fitting the experimental breakthrough data to the deactivation model, combining the adsorption of VOCs and the deactivation of GAC. The adsorption isotherm, and adsorbed amount and adsorption heat of VOCs were obtained using the breakthrough curve: the former for comparison with the conventional isotherm models, the latter for correlation with the physical properties of VOCs.

Key words: Adsorption, VOCs, Activated Carbon, Breakthrough Curve, Deactivation Model

INTRODUCTION

Granular activated carbon (GAC) [1] has long been used to treat effectively industrial gas streams containing volatile organic compounds (VOCs) to adsorb them onto GAC. Various contacting devices are available for adsorption systems, such as batch adsorbers and fixed bed adsorbers. The accurate design of the adsorber is achieved by developing a mass transfer model, which adequately describes the kinetics and mechanisms of the adsorption process. A plug-flow heterogeneous surface diffusion model [2] has been developed for representing axial dispersed plug-flow, external mass transfer, adsorption equilibrium on the fluid-particle interface, and intraparticle diffusion for a fixed-bed adsorption column. It is complicated to analyze the experimental breakthrough data in a fixed bed, because reasonable diffusivity [3,4] of a solute and physical properties of solid particle need to be known. The conventional isotherm models [2,5], such as the Langmuir, Freundlich, Brunauer-Emmett-Teller (BET), and Dubinin-Radushkevich-Kagener (DRK) model, have been used to obtain the adsorption kinetics, but it is difficult and tedious to prepare the experimental adsorption isotherm. Conversely, the deactivation model (DM) [6-8], as a simplified model, has been used to predict the breakthrough curve, assuming that the formation of a dense product layer over the surface of the adsorbent changed the number of active sites and the possible variations in the adsorption of active sites to cause a drop in the adsorption rate. This model makes the breakthrough curve analyzed easily and correlated with adsorption isotherm. Park et al. have investigated the adsorption kinetics from analysis of the experimental breakthrough data in a fixed bed using DM: adsorption of toluene vapor onto GAC [9], carbonation of sodium carbonate [10], potassium carbonate [11], and rubidium carbonate [12] with CO_2 To our knowledge, no literature report about the adsorption kinetics of VOCs onto GAC by analyzing the experimental breakthrough data using DM has yet been published except VOCs of trichloroethylene [7] and toluene vapor [9].

In this study, which is one of the series of works [9-12], the adsorption kinetics of several VOCs were obtained from analysis of the experimental breakthrough data using DM to obtain the adsorption capacity of GAC and heat adsorption of VOCs. Used VOCs were methanol, ethanol, methyl ethyl keton (MEK), benzene, n-propanol, toluene, and o-xylene.

THEORY

The formation of a dense product layer over the solid adsorbent creates an additional diffusion resistance and is expected to cause a drop in the adsorption rate. One would also expect it to cause significant changes in the accessible pore volume, active surface area, and activity per unit area of solid adsorbent with respect to the extent of the adsorption. All of these changes cause a decrease of vacant surface area of the adsorbent with time. In DM, the effects of all of these factors on the diminishing rate of VOC capture are combined in a deactivation rate term.

With assumptions [12] of the pseudo-steady state and the isothermal species conservation equation of adsorbate in the fixed bed is

$$-Q_o\frac{dC_A}{dS}-k_oC_A\alpha=0 \tag{1}$$

In writing this equation, axial dispersion in the fixed bed and any mass transfer resistances are assumed to be negligible.

According to the proposed DM, the rate of activity is expressed as

$$-\frac{d\alpha}{dt}=k_dC_A^n\alpha^m \tag{2}$$

†To whom correspondence should be addressed.
E-mail: swpark@pusan.ac.kr

The zeroth solution of the deactivation models is obtained by taking n=0. m=1, and the initial activity of adsorbent as unity.

$$a=\exp[-k_o\tau\exp(-k_dt)] \quad (3)$$

Eq. (3) is identical to the breakthrough equation proposed by Suyadal et al. [7] and assumes a fluid phase concentration that is independent of deactivation processes along the adsorber. More realistically, one would expect the deactivation rate to be concentration-dependent and, accordingly, axial-position-dependent in the fixed bed.

To obtain the analytical solution of Eq. (1) and (2) by taking n=m=1, an iterative procedure is applied. The procedure used here is similar to the paper proposed by Dogu [13] for the approximate solution of nonlinear equations. The zeroth solution of Eq. (3) is substituted into Eq. (2), and the first correction for the activity is obtained by the integration of this equation. Then, the corrected activity expression is substituted into Eq. (1), and integration of this equation gives the first corrected solution for the breakthrough curve.

$$a=\exp\left[\frac{[1-\exp(k_o\tau(1-\exp(-k_dt)))]}{1-\exp(-k_dt)}\exp(-k_dt)\right] \quad (4)$$

This iterative procedure can be repeated for further improvement of the solution. In this procedure, higher-order terms in the series solutions of the integrals are neglected. The breakthrough curve for the deactivation model with two parameters (k_o and k_d) is calculated from the concentration profiles by Eq. (4).

EXPERIMENTAL

1. An Apparatus for VOCs Capture and its Operation

Adsorption experiment (Fig. 1) used in this study was carried out in the presence of VOCs with GAC adsorbent in a fixed bed of a pyrex-glass adsorber with internal diameter of 0.02 m, which were the same as those of Park et al. [12]. Organic liquid was fed to the adsorber through the line heated by using a micro syringe pump (KD Scientific Co., Model; KDS 230, minimum flow rate; 2.7×10^{-9} m^3/h) within the range of 60×10^{-9} m^3/h-250×10^{-9} m^3/h at 298 K. Experiments were carried out at flow rates of nitrogen were within the range of 60×10^{-6}-150×10^{-6} m^3/min (measured at 298 K and adsorption temperature of 298-323 K with GAC of 0.002 kg. Experiments were repeated three times to obtain the average value of the adsorption kinetics. The concentrations of VOCs in the nitrogen stream at the inlet and outlet of the adsorber were measured by a gas chromatograph. The gas chromatograph (detector: thermal conductivity detector; column: SE-30 of 10 feet by 1/8 inch diameter of stainless steel; detector temperature: 190 °C; feed temperature: 190 °C; flow rate of He: 25.7 cm^3/min; retention time of N_2, n-propanol vapor as an example: 1.065, 1.535 min, respectively) connected to the adsorber allowed for on-line analysis of VOCs and N_2.

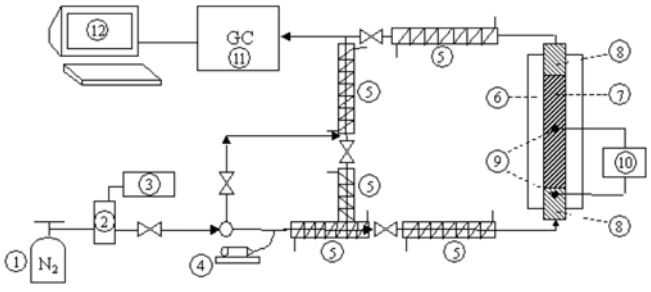

Fig. 1. Schematic diagram of a fixed bed apparatus.

1. Gas bomb	7. Sample
2. Mass flow controller	8. Glass wool
3. Flow indicator	9. Temperature probe
4. Micro syringe	10. Temperature controller
5. Heating line	11. GC (gas chromatography)
6. furnace	12. Personal computer

GAC particles were supported by glass wool from both sides. The adsorber was placed into a tubular furnace equipped with a temperature controller to maintain the constant temperature. The length of the fixed adsorbent section of the bed was 0.05 m of the adsorber. Temperature profiles were not observed within this section. All of the flow lines between the adsorber and the gas analyzer were heated to eliminate any condensation of VOCs. Three-way valves placed before and after the adsorber allowed for flow of the gaseous mixture through the bypass line during flow rate adjustments. Composition of the inlet stream was checked by the analysis of the stream flowing through the bypass line at the start experiments. The experimental procedure used to obtain the breakthrough curve of VOCs was the same as that reported in detail previously [12].

2. Materials

Adsorbent used in this study was granular activated carbon manufactured domestically (Samchully Activated Carbon Ltd., Korea) company. Prior to use, GAC was leached with boiling water for 24 hours, dried by heating at 378 K, and then, stored in a desiccator to be used in the adsorption experiments. The average size of adsorbent particle (3.51 mm) was measured in the range of 0.575-5.6 mm with a sieve analyzer; its bulk density (485 kg/m^3), by a conventional method using a pycnometer. Specific surface area, total pore volume, and average pore diameter were measured using BET technique (Micromeritics; ASAP 2000), and their values were 804.6 m^2/g, 0.4734 cm^3/g, 23.54 Å, respectively. Methanol, ethanol, MEK, benzene, n-propanol, toluene, and o-xylene were of reagent grade from Aldrich Chemicals and were used without further purification. Purity of nitrogen gas was greater than 99.9%.

RESULTS AND DISCUSSION

1. Kinetics of VOCs Adsorption on GAC

To investigate the adsorption kinetics of VOCs on GAC, adsorbed amount (q), and heat of adsorption (H_{AD}), the breakthrough curves of VOCs were measured according to change of the experimental variables such as flow rate (Q_g) of carrier gas, flow rate (Q_L) of VOC liquid, and adsorption temperature (T). Because the concentration (C_{Ao}) of VOC vapor at the inlet of the column depended on Q_g and Q_L, Q_L was adjusted using Q_g to keep up with fixed C_{Ao}. For example, Q_L of n-propanol for Q_g of 150×10^{-6} m^3/min was 165×10^{-9} m^3/h at a given C_{Ao} of 6,000 ppmv.

1-1. Effect of Flow Rate of VOCs-rich Gas

To investigate the effect of Q_o on the kinetics, the breakthrough curves of VOCs were measured according to the change of Q_g. The concentration of n-propanol vapors was measured against the adsorption time at various Q_g of 60×10^{-6}, 90×10^{-6}, 120×10^{-6}, and 150×10^{-6} m^3/min (measured at 298 K) and Q_L of 66×10^{-9}, 99×10^{-9}, 132×10^{-9}, and 165×10^{-9} m^3/h under the typical experimental conditions

such as W_o=0.002 kg, T=303 K, and C_{Ao}=6,000 ppmv, and plotted in Fig. 2.

As shown in Fig. 2, a shift of breakthrough curves to shorter times was observed at a greater flow rate of the gaseous mixture with a decrease in the amount of VOC that the bed can hold up to a certain breakthrough level. This result means that the adsorbed amount of VOC decreases as the space time of the gaseous mixtures in the fixed bed decreases. The k_o and k_d were evaluated by fitting the experimental breakthrough data to Eq. (4) by using a nonlinear least squares technique, and they were 1.347×10^{-7} m/min and 0.102 m^3/kmol·min, respectively. The concentration at the outlet was calculated from Eq. (4) using these values and drawn as solid lines in Fig. 2 with r^2 more than 0.999.

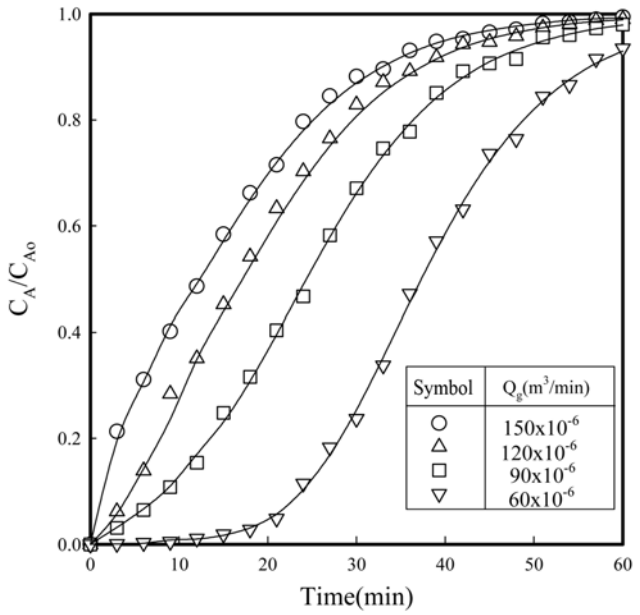

Fig. 2. Breakthrough curve of n-propanol vapors for various flow rates of N_2 (W_o=0.002 kg; T=303 K; $Q_L=132\times10^{-9}$ m^3/h; C_{Ao}= 6,000 ppmv).

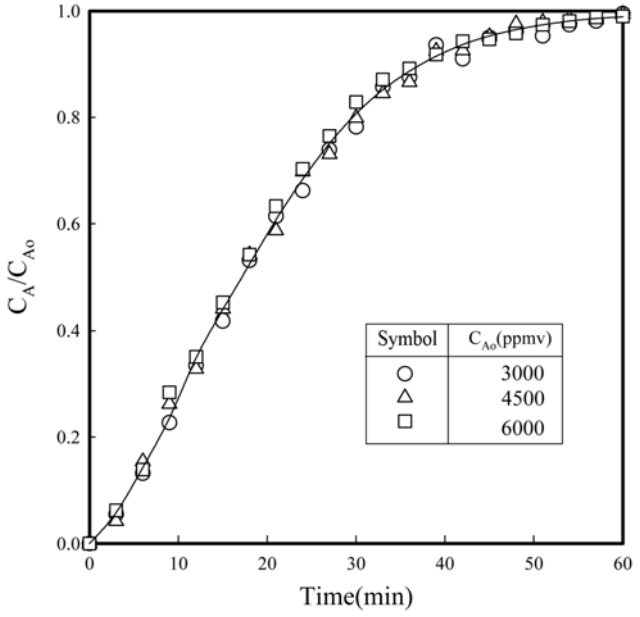

Fig. 3. Breakthrough curves of n-propanol vapors for various feedstock concentrations of n-propanol vapor ($Q_g=120\times10^{-6}$ m^3/min; T=303 K; W_o=0.002 kg).

1-2. Effect of Feedstock Concentration of VOC

To investigate the effect of C_{Ao} on the adsorption kinetics, the breakthrough curves of VOCs were measured at various Q_L of 66×10^{-9}, 99×10^{-9}, 132×10^{-9} cm^3/h, which were equivalent to C_{Ao} of 3,000, 4,500, 6,000 ppmv, respectively, under the typical experimental conditions such as VOC=n-propanol, $Q_g=120\times10^{-6}$ m^3/min, W_o=0.002 kg, and T=303 K. As shown in Fig. 3, the measured dimensionless concentrations of n-propanol were the same as each other with standard deviation of 0.007, and this result is due to expression of the dimensionless concentration form. Also, the calculated concentrations, using k_o of 1.347×10^{-7} m/min and k_d of 0.102 m^3/kmol·min, approached the measured ones with r^2 of 0.997.

1-3. Effect of Adsorption Temperature

To investigate the effect of adsorption temperature on the adsorp-

Table 1. k_o and k_d in adsorption of VOCs onto the activated carbon

VOCs	T (°C)	Vapor pressure (atm)	$k_o\times10^7$ (m/min)	k_d (m^3/kmolmin)	q (mg/g)
Methanol	25	0.1663	0.146	0.056	10.6
Ethanol		0.0773	0.371	0.102	15.9
MEK		0.1187	0.393	0.129	24.3
Benzene		0.1252	0.486	0.117	27.5
n-Propanol		0.0314	1.234	0.081	30.3
Toluene		0.0374	1.816	0.072	59.2(294*)
o-Xylene		0.0067	5.258	0.025	90.4
Methanol	30	0.2148	0.182	0.091	10.5
Ethanol		0.1028	0.425	0.153	15.6
MEK		0.1501	0.463	0.186	24.1
Benzene		0.1570	0.515	0.147	27.2
n-Propanol		0.0430	1.345	0.102	29.1
Toluene		0.0482	2.045	0.099	55.2
o-Xylene		0.0119	5.628	0.032	89.4
Methanol	40	0.3482	0.236	0.202	10.5
Ethanol		0.1763	0.563	0.387	15.2
MEK		0.2336	0..594	0.374	24.0
Benzene		0.2405	0.639	0.245	27.0
n-Propanol		0.0750	1.690	0.174	27.0
Toluene		0.0778	2.426	0.165	48.6
o-Xylene		0.0249	6.532	0.044	87.6
Methanol	50	0.5454	0.280	0.891	10.4
Ethanol		0.2907	0.661	1.158	15.2
MEK		0.3516	0.703	0.879	23.9
Benzene		0.3570	0.826	0.530	26.7
n-Propanol		0.1232	2.053	0.349	24.4
Toluene		0.1212	3.024	0.313	42.8
o-Xylene		0.0421	8.142	0.061	83.2

*: [14]

tion kinetics, the breakthrough curves were measured in the range of temperature from 298-323 K. The measured outlet concentrations of n-propanol were plotted against the adsorption time for the various temperatures indicated as various symbols in Fig. 5 under the typical experimental conditions (Q_g=120×10^{-6} m^3/min, W_o=0.002 kg, Q_L=132×10^{-9} m^3/h). The k_o and k_d were evaluated and tabulated in Table 1. The results in Fig. 4 indicated a shift in breakthrough curves toward the right with decreased temperature, which might be attributed to an increase in the amount of adsorbed VOC. The activation energy of the adsorption (ΔE_A) and deactivation energy (ΔE_D) were obtained from Arrhenius plots shown in Fig. 5 and their values were 16.6 and 46.6 kJ/mole, respectively.

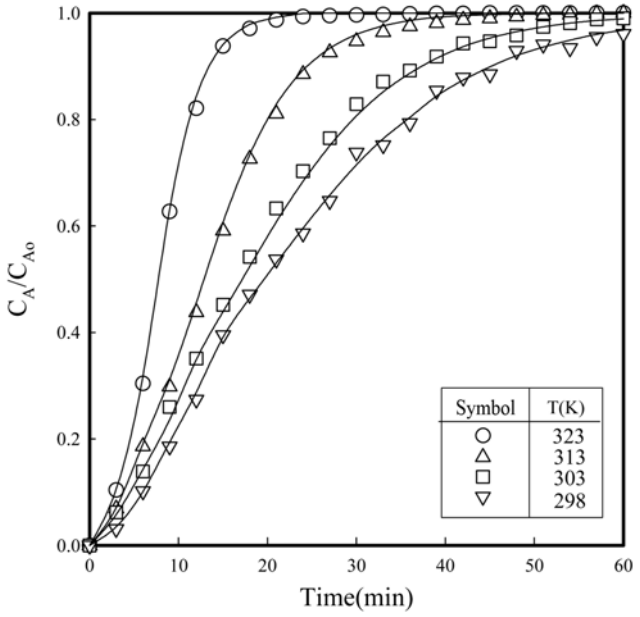

Fig. 4. Breakthrough curves of n-propanol vapors for various temperatures (Q_g=120×10^{-6} m^3/min; W_o=0.002 kg; Q_L=132×10^{-9} m^3/h; C_{Ao}=6,000 ppmv).

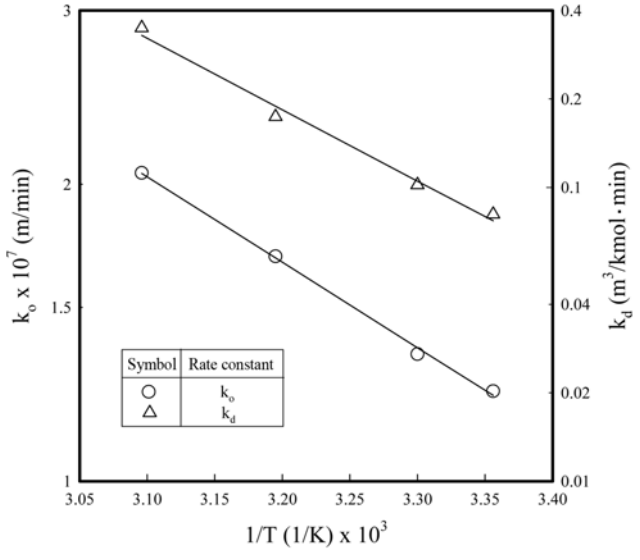

Fig. 5. Effect of temperature on adsorption rate constant and deactivation rate constant for n-propanol vapor (Q_g=120×10^{-6} m^3/min; W_o=0.002 kg; Q_L=132×10^{-9} m^3/h; C_{Ao}=6,000 ppmv).

Table 2. E_A and E_D in adsorption of VOCs on the activated carbon

VOCs	Molecular weight	Boiling point (°C)	ΔE_A (kJ/mol)	ΔE_D (kJ/mol)
Methanol	32	64.7	20.4	86.2
Ethanol	46	78.4	18.3	77.8
MEK	72	79.6	18.5	60.9
Benzene	78	80.1	17.2	47.9
n-Propanol	60	97.8	16.6	46.6
Toluene	92	110.6	16.0	46.3
o-Xylene	106	144.4	13.9	27.9

The values of k_o and k_d, obtained at various VOCs and temperatures, and DE_a and DE_d are in Table 1 and Table 2, respectively. The values of k_o and k_d of toluene vapor in Table 1 coincided with those in Park et al. [9].

1-4. Comparison of the Proposed Models

Several equilibrium models [5], which have been developed to describe adsorption isotherm relationships, are useful for describing adsorption capacity and theoretical evaluation of thermodynamic parameters, such as heats of adsorption. But, sometimes the experimental procedure to prepare the adsorption isotherm relationships is very tedious and time consuming. The equilibrium concentrations between two phases, which are used to describe adsorption isotherm relationships, can be obtained by Eq. (5) and (6), where a(t), x and y are the dimensionless concentrations of VOC in the breakthrough data, in the gas phase and solid phase, respectively. The equilibriums for single-solute adsorption given in the literature [5] are frequently presented as dimensionless concentration isotherms.

$$x = \frac{\int_0^t a(t)dt}{\int_0^\infty a(t)dt} \tag{5}$$

$$y = \frac{t - \int_0^t a(t)dt}{\int_0^\infty dt - \int_0^\infty a(t)dt} \tag{6}$$

To compare the deactivation model with the equilibrium isotherm models, models selected by Suyadal et al. [7] were used as follows: Langmuir, Freundlich, BET, and DRK model, whose formulas were listed in Table 3.

The typical experimental conditions of VOC=n-propanol, Q_g=120×10^{-6} m^3/min, W_o=0.002 kg, T=303 K, Q_L=132×10^{-9} m^3/h and C_{Ao}=6,000 ppmv were used. Using a(t) obtained from the experimental parameters, the values of x and y obtained from Eq. (5) and (6), are shown in Fig. 6 and used to obtain to give the constants of a and b in each model.

As shown in Fig. 6 and Table 3, the proposed deactivation model fitted the data with the highest correlation (r^2) of 0.999, and the adsorption of n-propanol on GAC might be favorable isotherms due to the separation factor less than unity. The equilibrium relation in other VOCs presented similar results as shown in Fig. 6.

The BET model is an extended model of the Langmuir model and includes multi-layer adsorption phenomena. BET has assump-

Table 3. Selected adsorption isotherms to fit the breakthrough data of n-propanol vapor for comparison with the deactivation model

Adsorption isotherms	Mathematical representation of adsorption isotherms	Linearized forms	Parameters and correlation coefficient
Langmuir	$y=\frac{ax}{(1+bx)}$	$\frac{1}{y}=\frac{1}{ax}+\frac{b}{a}$	a=7.0137 b=7.2685 r^2=0.976
Freundlich	$y=ax^b$	$\ln(y)=\ln(a)+b\ln(x)$	a=1.0991 b=0.5179 r^2=0.981
Brunauer-emmett-teller	$y=\frac{x}{(1-x)(a+bx)}$	$\frac{x}{y(1-x)}=a+bx$	a=−1.170 b=8.3097 r^2=0.362
Dubinin-radshkevich-kagener	$y=a\exp[-b\ln^2(x)]$	$\ln(y)=\ln(a)-b\ln^2(x)$	a=0.8289 b=0.1278 r^2=0.968
Deactivation model (this study)	x According to eq. (5) y According to eq. (6)		$k_s\tau$=1.763 k_d=0.102 r^2=0.999

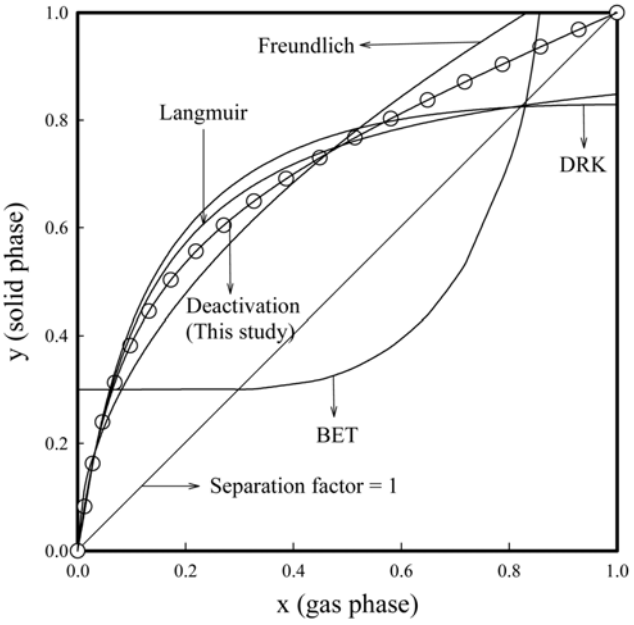

Fig. 6. Comparison of the model in describing the experimental breakthrough curve of n-propanol vapors according to Table 3 (Q_g=120×10^{-6} m^3/min; T=303 K; W_o=0.002 kg; Q_L=132×10^{-9} m^3/h; C_{Ao}=6,000 ppmv).

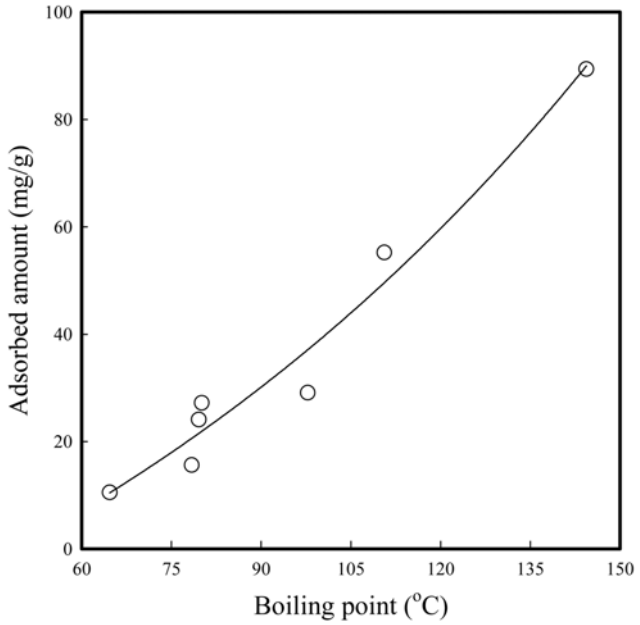

Fig. 7. Dependence of adsorbed amount of VOCs at 303 K on boiling point (q=−71.14+46.96e$^{-0.0085Bp}$ with r^2=0.988 and se= 6.23).

tions that any given layer need not be completed before subsequent layers can form, that the first layer of molecules adheres to the surface with a comparable energy to the heat of adsorption for monolayer attachment, and that subsequent layers are essentially condensation reactions [8]. As shown in Fig. 6, the BET model was not fitted with the experimental data. From this result, the practical adsorption situation in this study may not be the multi-layer adsorption phenomena.

2. Adsorption Capacity of GAC

To compare the adsorption capacity of GAC for various species of VOCs, the adsorbed amount of VOCs on GAC was obtained by using the breakthrough curve as follows [6]:

$$q=\frac{C_{Ao}Q_o}{W_oM_w}\left[t-\int_0^t a(t)dt\right] \quad (7)$$

The adsorbed amounts, using the breakthrough curve and Eq. (7) for various VOCs and under the conditions of Q_g=120×10^{-6} m^3/min, W_o=0.002 kg, Q_L=132×10^{-9} m^3/h, and C_{Ao}=6,000 ppmv are tabulated Table 1. Lim et al. [14] adsorbed toluene vapor in a fixed-bed activated carbon column using 2 g of AC during 1,000 min at 20 °C and obtained the adsorbed amount (294 mg/g) of toluene vapor on AC, presented in Table 1. The difference between their value and ours may be due to the different physical properties of AC and

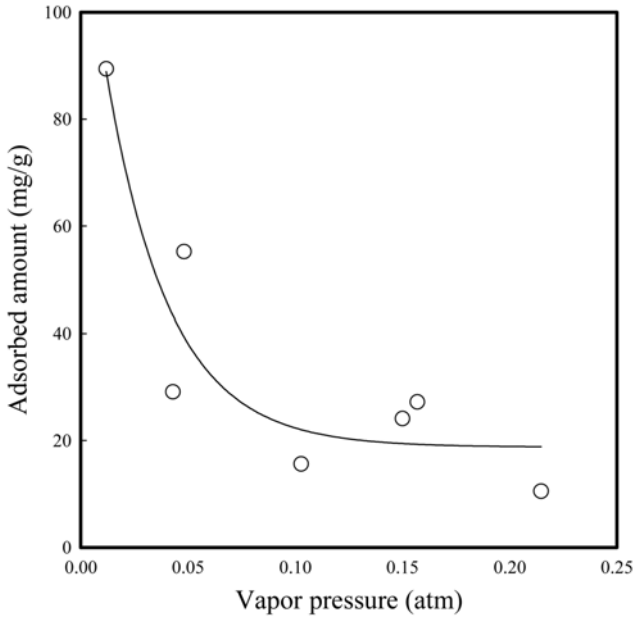

Fig. 8. Dependence of adsorbed amount of VOCs on vapor pressure at 303 K ($q=18.87+108.39e^{-33.7532P_o}$ with $r^2=0.978$ and se=9.84).

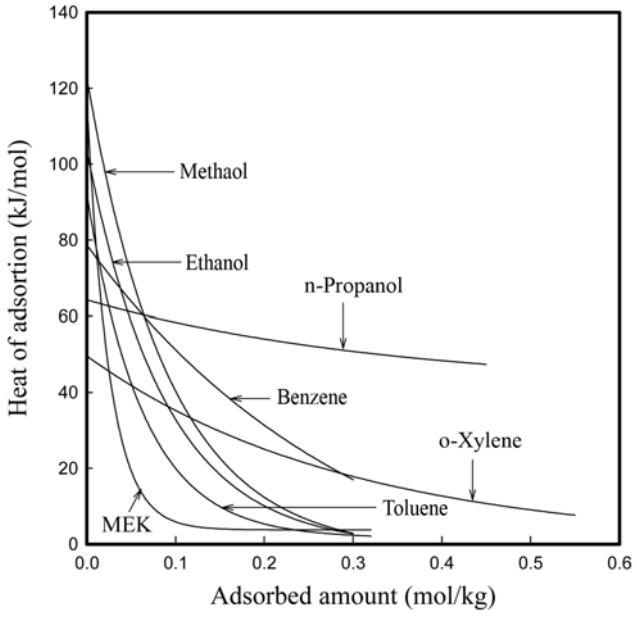

Fig. 9. Isosteric heat of adsorption for VOCs on GAC at 303 K.

adsorption time and temperature each other.

To observe the effect of adsorbed amounts on physical properties of the adsorbate, the adsorbed amounts in Table 1 were plotted against the boiling point and vapor pressure at 303 K in Fig. 7 and 8, respectively. The vapor pressures of VOCs obtained from Antoine equation [14] for various temperatures and boiling point are tabulated in Table 1 and 2, respectively.

As shown in Figs. 7 and 8, the adsorbed amount increases with increasing the boiling point with empirical formulas of $q=-71.14+49.96e^{-0.0082Bp}$ with $r^2=0.988$ and decreasing the vapor pressure of $q=18.87+108.39e^{-33.2546Po}$ with $r^2=0.978$, respectively. These trends are due to the decrease of volatility by increase of the boiling point or decrease of the vapor pressure. These trends are similar to those in Lim et al. [14].

3. Heat of Adsorption

When an adsorbent adsorbs one or more adsorbates, adsorption heat is usually generated since all adsorption processes are exothermic. Eventually, the evolved affects the adsorption performance considerably. If the adsorption system was very ideal following the Langmuir isotherm, the heat of adsorption would be independent of the amount adsorbed. However, it would not be true for most adsorption processes because of the energetically heterogeneous surfaces of adsorbents. The isosteric heat of adsorption (H_{AD}) may be evaluated simply by applying the Clausius-Clapeyron equation if one has a good set of adsorption equilibrium data obtained at several temperatures [16] as follows:

$$\frac{H_{AD}}{RT^2}=\frac{\partial \ln(P/P_o)}{\partial T} \tag{8}$$

$\ln(P/P_o)$ at each temperature was obtained from relationship of x and y by DM using parameter of q, and then, H_{AD} was estimated using Eq. (8) and slope of plots of $\ln(P/P_o)$ vs. temperature. Under

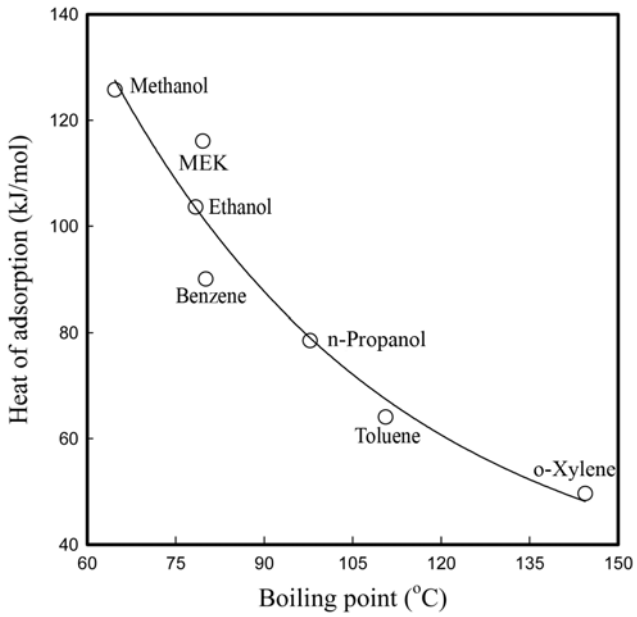

Fig. 10. Dependence of heat of adsorption on boiling point of VOCs ($H_{AD}=302.74e^{-0.0136Po}$ with $r^2=0.994$ and se=8.32).

the conditions of $Q_g=120\times10^{-6}$ m^3/min, $W_o=0.002$ kg, $Q_L=132\times10^{-9}$ m^3/h, $C_{Ao}=6{,}000$ ppmv, and 303 K, H_{AD} for various VOCs are shown in Fig. 9.

H_{AD} of adsorbates, except n-propanol and o-xylene, decreases almost exponentially with the adsorption amount. This result is quite natural since the adsorption occurs primarily on sites with higher energy. In Fig. 9, the magnitude of H_{AD} at initial adsorption (q=0) is methanol>ethanol>MEK>benzene>n-propanol>toluene>o-xylene. Kim et al. [16] presented the heat of adsorption for solvents on AC with adsorption equilibrium using a quartz spring balance, and its value was about 1,600 kJ/mol of MEK and 400 kJ/mol of toluene

at adsorbed amount of 0.1 mol/kg. These heats of adsorption were very much larger than those in Fig. 9. The big differences between their value and ours may be due to the different physical properties of AC and adsorption time and temperature each other.

To observe the relationship between H_{AD} and the physical properties of VOCs, H_{AD} at q=0 are plotted against the boiling point of VOCs in Fig. 10.

As shown in Fig. 10, H_{AD} decreases with increasing the boiling point with empirical formulas of $H_{AD}=302.74e^{-0.0136Bp}$ with $r^2=0.994$ and se=8.32. These trends are due to decrease of volatility by increase of the boiling point or decrease of the vapor pressure.

CONCLUSIONS

The breakthrough data for adsorption of VOC vapor such as meth- and o-xylene on an adsorbent of granular activated carbon were measured in a fixed bed to observe the adsorption kinetics. The deactivation model was used to evaluate the adsorption kinetics of the adsorption rate constant and deactivation rate constant by fitting the experimental breakthrough data with the model by using a nonlinear least squares technique. The experimental breakthrough data fitted with the deactivation model could be used to obtain the adsorption isotherm, the adsorbed amount, and heat of adsorption. The proposed deactivation model fitted the data very well among the adsorption isotherms. The adsorbed amount and heat of adsorption were related to the boiling points and vapor pressure of the VOCs. The adsorbed amount increases and heat of adsorption decreases with increasing the boiling point exponentially.

ACKNOWLEDGMENTS

This work was supported by Brain Korea 21 Project and a grant (2006CCD11P011A-21-3-010) from the Energy Technology R&D of Korea Energy Management Corporation. Dae-Won Park is also thankful for KOSEF (R01-2007-000-10183-0).

NOMENCLATURE

a : dimensionless concentration (C_A/C_{Ao}) of CO_2 in the breakthrough data
B_p : boiling point of VOC [°C]
C_A : concentration of VOC in gas phase [kmol/m^3]
C_{Ao} : inlet concentration of VOC in gas phase [kmol/m^3]
E_A : activation energy of the adsorption [kJ/mol]
E_D : activation energy of the deactivation [kJ/mol]
H_{AD} : heat of adsorption [kJ/mol]
k_o : adsorption rate constant [m/ min]
k_d : deactivation rate constant [m^3/kmol·min]
m : reaction order with respect to α
M_w : molecular weight [kg/kmol]
n : reaction order with respect to C_A
P_o : vapor pressure of VOC [atm]
q : adsorbed amount of adsorbate [mg/g] or [mol/kg]
Q_g : volumetric flow rate of nitrogen [m^3/min]
Q_L : volumetric flow rate of VOC liquid being fed into the micro syringe [m^3/h]
Q_o : volumetric flow rate of gaseous mixture [m^3/min]
R : gas law constant 8.314 [J/mol·K]
r^2 : correlation coefficient
S : vacant surface area of the adsorbent [m^2]
se : standard error
S_o : specific initial vacant surface area of the adsorbent [m^2/kg]
t : adsorption time [min]
T : adsorption temperature [K]
W_o : amount of the adsorbent [kg]
x : dimensionless concentrations in the gas phase through adsorption isotherm
y : dimensionless concentrations in the solid phase through adsorption isotherm

Greek Letters

α : activity of the adsorbent [-]
τ : surface time defined as W_oS_o/Q_o [min/m]

Subscripts

A : vapor of VOC

REFERENCES

1. R. T. Yang, *Gas separation by adsorption processes*, Butterworth, Boston (1987).
2. D. W. Ruthven, *Principles of adsorption and adsorption processes*, John & Wiley, New York (1984).
3. L. K. Doraiswamy and M. M. Sharma, *Heterogeneous reactions*, John Wiley & Sons, New York (1954).
4. N. Orbey, G. Dogu and T. Dogu, *Can. J. Chem. Eng.*, **60**, 314 (1982).
5. M. Suzuki, *Adsorption engineering*, Kodansga Ltd., Tokyo (1990).
6. S. Yasyerli, T. Dogu, G. Dogu and I. Ar, *Chem. Eng. Sci.*, **51**, 2523 (1996).
7. Y. Suyadal, M. Erol and M. Oguz, *Ind. Eng. Chem. Res.*, **39**, 724 (2000).
8. T. Kopac and S. Kocabas, *Chem. Eng. Comm.*, **190**, 1041 (2003).
9. S. W. Park, B. S. Choi and J. W. Lee, *Sep. Sci. Technol.*, **42**, 2221 (2007).
10. S. W. Park, D. H. Sung B. S. Choi and K. W. Oh, *Sep. Sci. Technol.*, **41**, 2665 (2006).
11. S. W. Park, D. H. Sung, B. S. Choi, J. W. Lee and H. Kumazawa, *J. Ind. Eng. Chem.*, **12**, 522 (2006).
12. K. S. Hwang, S. W. Park, D. W. Park, K. J. Oh and S. S. Kim, *Korean J. Chem. Eng.*, **26**(4) (2009).
13. T. Dogu, *Am. Inst. Chem. Eng. J.*, **32**, 849 (1986).
14. J. K. Lim, S. W. Lee, S. K. Kim, D. K. Lee and M. G. Lee, *J. Environmental Sci.*, **14**, 61 (2005).
15. R. C. Reid, J. M. Prausnitz and B. E. Poling, *The properties of gases & liquids*, 4th Ed., McGraw-Hill Book Co., New York (1987).
16. D. Kim, W. G. Shim and H. Moon, *Korean J. Chem. Eng.*, **18**(4), 518 (2001).